Research Paper
Computational Methods for Differential Equations
http://cmde.tabrizu.ac.ir
Vol. *, No. *, *, pp. 1-15
DOI:10.22034/cmde.2024.60950.2607

Analysis of quarantine and liberate effects on viral infection using SEIR and Caputo α-fractional-order model

Akbar Dehghan Nezhad* **and Arezoo Moslemi Ghadikolaei**
School of Mathematics and Computer Science, Iran University of Science and Technology, Narmak, Tehran, 1684613114, Iran.

Abstract

Of the various control measures available, lockdown is widely considered to be the most reliable method for containing the spread of the Coronavirus. This study presents two mathematical models utilizing $\boldsymbol{\alpha}$-fractional derivatives to investigate the significance of lockdown in reducing the spread of the virus. In this article, the entire population is divided into four groups:
1) The first group comprises the susceptible population who are not under lockdown.
2) The second group consists of susceptible individuals who are under lockdown.
3) The third group comprises infected individuals who are not under lockdown.
4) The fourth group consists of infective individuals who are under lockdown.
One of the aforementioned methods examines this disease by generalizing the SEIR $\boldsymbol{\alpha}$-fractional derivatives. The second model comprises five nonlinear differential equations of $\boldsymbol{\alpha}$-fractional order. In both methods, $\boldsymbol{\alpha} = (\alpha_1, \cdots, \alpha_n)$, where $0 < \alpha_i \leq 1$ for every $1 \leq i \leq n$. In other words, if $\mathbb{T} = (0, 1]$, then $\boldsymbol{\alpha} \in \mathbb{T}^n$.

Keywords. Lockdown, Coronavirus, Mathematical models, $\boldsymbol{\alpha}$-fractional.
2010 Mathematics Subject Classification. 92D30.

1. Introduction

A pandemic is characterized by the widespread occurrence of an infectious disease, affecting a large geographic area such as multiple continents or globally, and impacting a significant number of people. Diseases that are endemic and prevalent, with a consistent number of cases over time, like seasonal influenza, are typically not classified as pandemics since they occur in large regions simultaneously rather than spreading worldwide. Over the past 50,000 to 100,000 years, as human populations have increased and spread globally, new viral infectious diseases have emerged [7]. In ancient times, when human settlements were small and isolated, epidemic diseases were rare. However, around 11,000 years ago, smallpox, caused by the variola virus, emerged among agricultural communities in India, eventually becoming one of the deadliest viral infections in history [2].

The concept of quarantine, as it is understood today, originated in the 14th century as a measure to prevent the spread of plague epidemics to coastal cities. Ships arriving in Venice from infected ports were required to anchor for 40 days before docking, a practice known as quarantine, derived from the Italian words "quaranta giorni" meaning 40 days. The plague, caused by Yersinia pestis bacteria transmitted by fleas, has caused several pandemics throughout history [11].

Moreover, the Caputo fractional order has been explored for its ability to model non-local behavior, potentially offering advantages over integer-order models [1, 5, 6, 8, 9, 12, 14].

In a recent study by Khan et al. [5, 6], the α-fractional order model was examined to elucidate the interaction between unknown hosts and bats, which has implications for understanding diseases' origins, such as COVID-19. Similarly, Yu et al. [14] developed a fractional time delay dynamics model to predict localized outbreaks of COVID-19, while Xu et al. [13] proposed a generalized fractional-order SEIQRD model to forecast future outbreaks of

Received: 19 March 2024 ; Accepted: 28 September 2024.
* Corresponding author, Email: dehghannezhad@iust.ac.ir .

infectious diseases, including COVID-19. Additionally, Shaikh et al. [10] utilized a model called Batshosts reservoir people transmission fractional order COVID-19 to evaluate prevention measures, predict future outbreaks, and explore control strategies.

Various models have been employed to analyze the dynamics of COVID-19, including predicting susceptible individuals in a population. However, to our knowledge, none have specifically assessed the effectiveness of targeted lockdown measures, and most have utilized integer-order models.

This article is structured as follows:

(1) Section 2 provides preliminary definitions.
(2) In Section 3, we investigate the α-fractional order model for COVID-19.
(3) Section 4 discusses the non-negativity and boundedness of the model, as well as its uniqueness and existence.
(4) Section 5 focuses on the analysis and stability of the model, including the identification of possible fixed points and local stability analysis.
(5) Section 6 presents numerical schemes and simulations used in the study.
(6) Finally, Section 7 presents the conclusions drawn from our analysis.

2. Preliminaries

Definition 2.1. Assume that $\alpha > 0$ and $\xi \in L([0,b],\mathbb{R})$, where $[0,b] \subset \mathbb{R}^+$. For functions in the Riemann-Liouville sense, the fractional integral of order α is defined as

$$I^{\alpha}_{0^+}\xi(t) = \frac{1}{\Gamma(\alpha)}\int_0^t (t-x)^{\alpha-1}\xi(x)dx, \quad t>0\cdot \tag{2.1}$$

Here, $\Gamma(\cdot)$ denotes the classical gamma function, given by

$$\Gamma(\alpha) = \int_0^{\infty} x^{\alpha-1}\exp(-x)dx\cdot \tag{2.2}$$

Definition 2.2. Let $\xi : [0,b] \longrightarrow \mathbb{R}$ be a function. The Riemann-Liouville fractional derivative of order $\alpha \in \mathbb{R}^+$ is defined as follows

$$D^{\alpha}_{0^+}(\xi)(t) = \frac{1}{\Gamma(n-\alpha)}\frac{d^n}{dt^n}\int_0^t \frac{\xi(x)}{(t-x)^{\alpha-n+1}}dx, \quad \alpha\in[n-1,n), \quad n\in\mathbb{N}\cdot \tag{2.3}$$

Definition 2.3. The Caputo fractional derivative of a function $\xi : [0,b] \longrightarrow \mathbb{R}$ of order $\alpha \in \mathbb{R}^+$ is defined as follows

$${}^{C}D^{\alpha}_{0^+}(\xi)(t) = \frac{1}{\Gamma(n-\alpha)}\int_0^t \frac{\xi^{(n)}(x)}{(t-x)^{\alpha-n+1}}dx, \quad \alpha\in[n-1,n), \quad n\in\mathbb{N}\cdot \tag{2.4}$$

Riemann-Liouville and Caputo fractional derivatives are linear operators. However, most definitions of fractional derivatives, such as the Riemann-Liouville and Caputo fractional derivatives, do not possess the intrinsic features of the classical derivative. In 2014, R. Khalil presented a new definition of fractional derivatives, which encompasses all the main features of the derivative and is called conformable fractional derivatives [4].

Definition 2.4. Conformable fractional derivative (CFD) of the function $\xi : [0,\infty) \longrightarrow \mathbb{R}$ of order $\alpha \in [0,\infty)$ at $a \in [0,\infty)$ is defined as

$$D^{\alpha}\xi(a) = \lim_{h\longrightarrow 0}\frac{\xi(a+ha^{1-\alpha})-\xi(a)}{h}\cdot \tag{2.5}$$

In this work, the set of $\boldsymbol{x} = (x_1,\cdots,x_n) \in \mathbb{R}^n$ for which $x_i > 0$ for every $i = 1,\cdots,n$, is denoted by $\mathbb{R}^{n+}$. Let $\mathbb{T} = [0,1)$. Here and subsequently, $\mathbb{T}^n$ denotes the Cartesian product of n copies of $\mathbb{T}$, denoted as $\mathbb{T}\times\mathbb{T}\times\cdots\times\mathbb{T}$ (n times).

Let $AC^n(a,b)$ be the space of functions f which are absolutely continuous on $[a,b]$. For $n \in \mathbb{N} = \{1,2,3,\cdots\}$, the space $AC^n(a,b)$ is the set of complex-valued functions $f(X)$ which have continuous derivations up to order $n-1$ on $[a,b]$ such that $f^{(n-1)}(x) \in AC^n(a,b)$.

Lemma 2.5. *[3] Let $\alpha \in \mathbb{C}$ and $Re(\alpha) > 0$. Suppose $\xi \in AC^n(0,b)$ or $\xi \in C^n(0,b)$. Then, we have*

$$(I_{0+}^{\alpha}\, {}^{C}D_{0+}^{\alpha}\xi)(x) = \xi(x) - \sum_{k=0}^{n-1} \frac{\xi^{(k)}(a)}{k!}(x-a)^k. \tag{2.6}$$

In particular, if $\alpha \in \mathbb{T}$ and $\xi \in AC^n(0,b)$ or $\xi \in C^n(0,b)$, then

$$(I_{0+}^{\alpha}\, {}^{C}D_{0+}^{\alpha}\xi)(x) = \xi(x) - \xi(b). \tag{2.7}$$

Definition 2.6. Assume that $\Psi : \mathbb{R}^{n^+} \longrightarrow \mathbb{R}^m$ be a multi-variable vector-valued function such that

$$\Psi(x_1, ..., x_n) = (\Psi_1(x_1, ..., x_n), ..., \Psi_m(x_1, ..., x_n))$$

and $\boldsymbol{\alpha}(t) \in \mathbb{T}^n$. Let $\mho = (a_1 + h_1\delta(\alpha_1, a_1)a_1^{1-\alpha_1}, ..., a_n + h_n\delta(\alpha_n, a_n)a_n^{1-\alpha_n})$. Then the Ψ is $\boldsymbol{\alpha}$-differentiable at $\boldsymbol{a} \in \mathbb{R}^{n^+}$, if there is a linear transformation $L : \mathbb{R}^n \longrightarrow \mathbb{R}^m$ such that

$$\lim_{h\to 0} \frac{\|\Psi(\mho) - \Psi(a_1, ..., a_n) - L(h)\|}{\|h\|} = 0$$

where $h = (h_1, ..., h_n)$ where $\delta(\alpha_i, a)$ is a function that may depend on α_i and a. The linear transformation L is denoted by $D_{\delta}^{\boldsymbol{\alpha}}\Psi(a)$ and called the CD of Ψ of order $\boldsymbol{\alpha}$ ($\boldsymbol{\alpha}$-derivative of Ψ) at $\boldsymbol{a}$.

3. Mathematical model formulation

The total population is denoted as $N(t)$. Since a complete and universal lockdown has not been implemented in Iran. Therefore, the population is divided into four categories:

(1) The first category, represented by $S(t)$, includes susceptible individuals not subjected to lockdown.
(2) The second category, denoted as $S_L(t)$, consists of susceptible individuals under lockdown.
(3) The third category, labeled as $I(t)$, comprises infective individuals not under lockdown. Here, isolation serves as a substitute for lockdown for simplicity.
(4) The fourth category, indicated by $I_L(t)$, encompasses infective individuals under lockdown.

We use $L(t)$ to symbolize the cumulative density function of the lockdown program. The dynamics of these population categories can be described by a system of α-fractional order differential equations, presented below.

3.1. Parameters description.

In this subsection, we introduce several key parameters related to α-fractional order, supporting the analysis of the system.

(1) Recruitment is denoted by Λ.
(2) Infection contacts are represented by β.
(3) The imposition of lockdown on susceptible and infected individuals is defined by λ_1 and λ_2, respectively.
(4) Recovery rates for susceptible and infected individuals are denoted by γ_1 and γ_2, respectively.
(5) Death rates due to infection for susceptible and infected individuals are indicated by ν_1 and ν_2, respectively.
(6) The natural death rate is denoted by d.
(7) The rate of transfer of susceptible individuals from the lockdown class to the susceptible class is represented by θ_1.
(8) The rate of transfer of infected individuals from the lockdown class to the infected class is denoted by θ_2.
(9) μ represents the rate of implementation of the lockdown program.
(10) ϕ signifies the rate of depletion of the lockdown program.
(11) η denotes the death rate within each subclass.
(12) The rate of interaction between susceptible and infected populations is represented by i.
(13) $\mathcal{R}$ symbolizes the rate of recovery in the four classes.
(14) The rate at which the exposed class completes its incubation period and enters the infected class is denoted by ψ, while the removal or recovery rate of the infected class is represented by ω.

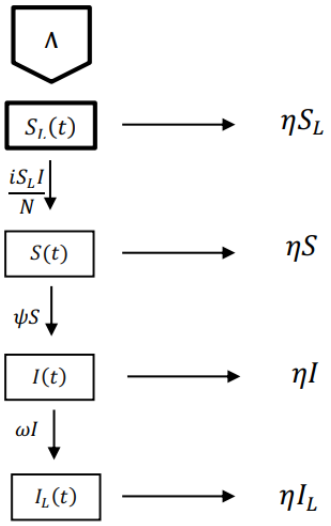

FIGURE 1. Flowchart of the given SEIR model [3].

Type 1. SEIR α-fractional-order model. The susceptible-exposed-infected-remove (SEIR) $\boldsymbol{\alpha}$-fractional-order model is obtained using the route $\frac{iS_L(t)I(t)}{N}$ as follows

$$\begin{cases} D^{\alpha}_{0^+}S(t) = \dfrac{iS_L(t)I(t)}{N} - \eta S(t) - \psi S(t), \\ D^{\alpha}_{0^+}S_L(t) = \Lambda - \eta S_L(t) - \dfrac{iS_L(t)I(t)}{N}, \\ D^{\alpha}_{0^+}I(t) = \psi S(t) - \eta I(t) - \omega I(t), \\ D^{\alpha}_{0^+}I_L(t) = \omega I(t) - \eta I_L(t), \end{cases} \tag{3.1}$$

where $\boldsymbol{\alpha} = (\alpha_1)$, $\alpha_1 \in \mathbb{T}^1$, and $\mathbb{T} = (0, 1]$. This model has the following non-negative initial conditions

$$S(0) = S^* \geq 0, \quad S_L(0) = S^*_L \geq 0, \quad I(0) = I^* \geq 0, \quad I_L(0) = I^*_L \geq 0\cdot \tag{3.2}$$

Type 2. Model of α-fractional-order including lockdown for COVID-19. By employing the aforementioned procedures for $\boldsymbol{\alpha} = (\alpha_1, \cdots, \alpha_n) \in \mathbb{T}^n$, $\alpha_i \in \mathbb{T}$, and $\mathbb{T} = (0, 1]$, we obtain the following model

$$\begin{cases} D^{\alpha_i}_{0^+}S(t) = \Lambda^{\alpha_t} - \beta^{\alpha_i}S(t)I(i) - \lambda_1^{\alpha_i}S(t)L(t) - d^{\alpha_i}S(t) + \gamma_1^{\alpha_i}I(t) + \gamma_2^{\alpha_i}I_L(t) + \theta_1^{\alpha_i}S_L(t), \\ D^{\alpha_i}_{0^+}S_L(t) = \lambda_1^{\alpha_i}S(t)L(t) - d^{\alpha_i}S_L(t) + \theta_1^{\alpha_i}S_L(t), \\ D^{\alpha}_{0^+}I(t) = \beta^{\alpha_i}S(t)I(t) - \gamma_1^{\alpha_i}I(t) - d^{\alpha_i}I(t) + \lambda_2^{\alpha_i}I(t)L(t) + \theta_2^{\alpha_i}I_L(t) - \nu_1^{\alpha_i}I(t), \\ D^{\alpha_i}_{0^+}I_L(t) = \lambda_2^{\alpha_i}I(t)L(t) - d^{\alpha_i}I_L(t) + \theta_2^{\alpha_i}I_L(t) - \gamma_2^{\alpha_i}I_L(t) - \nu_2^{\alpha_i}I_L(t), \\ D^{\alpha_i}_{0^+}L(t) = \mu^{\alpha_i}I(t) - \phi^{\alpha_i}L(t)\cdot \end{cases} \tag{3.3}$$

4. Establishing the non-negativity, boundedness, existence, and uniqueness of the model

4.1. **Non-negativity and boundedness of the first proposed model.** This subsection will provide confirmation of the boundedness and positivity of the system (3.1) Figure 1. In Lemma 4.1, we demonstrate the positivity of the model (3.1) Figure 1.

Lemma 4.1. *Suppose that $\Phi \subset \mathbb{R}\times\mathbb{C}^n$ is an open set and that $\Upsilon_j \in C(\Phi,\mathbb{R})$ for $j = 1, 2, \cdots$. If $\Upsilon_j|_{x_j(t)=0, X(t)\in\mathbb{C}^n_{0+}} \geq 0$ for every $j = 1, \cdots, n$ and $X_t = (x_{1t}, x_{2t}, \cdots, x_{nt})^T$, then the invariant domain of the equations*

$$D^{\alpha_i}_{0+} x_j(t) = \Upsilon_j(t, X_t), \quad t \geq \delta, j = 1, 2, \cdots, n, \tag{4.1}$$

is $\mathbb{C}^n_{0+}\{\varphi = (\varphi_1, \varphi_2, \cdots, \varphi_n) : \ \varphi \in C([-\nu, 0], \mathbb{R}^n_{0+})\}$, where

$$\mathbb{R}^n_{0+} = \{(x_1, x_2, \cdots, x_n) : \ x_j \geq 0, \ j = 1, 2, \cdots, n\}. \tag{4.2}$$

Proposition 4.2. *The system (3.1) is invariant in $\mathbb{R}^4_{0+}$.*

Proof. We can obtain

$$D^{\alpha}_{0+} X(t) = M(X(t)), \quad X(0) = X_0 \geq 0, \tag{4.3}$$

$$M(X(t)) = (M_1(X), M_2(X), M_3(X), M_4(X))^T. \tag{4.4}$$

by rewriting the system (3.1). It was observed that for $\boldsymbol{\alpha} = (\alpha_1, \cdots, \alpha_n)$, $\alpha_i \in \mathbb{T}$, and $\mathbb{T} = (0, 1]$,

$$\begin{cases} D^{\alpha_i}_{0+} S(t)|_{S=0} = \dfrac{iS_L(t)I(t)}{S_L(t) + I(t) + I_L(t)} \geq 0, \\ D^{\alpha_i}_{0+} S_L(t)|_{S_L=0} = \Lambda \geq 0, \\ D^{\alpha_i}_{0+} I(t)|_{I=0} = \psi S(t) \geq 0, \\ D^{\alpha_i}_{0+} I_L(t)|_{I_L=0} = \omega I(t) \geq 0. \end{cases} \tag{4.5}$$

Lemma 4.1 states that $\mathbb{R}^4_{0+}$ is an invariant set. □

Proposition 4.3. *The system (3.1) is bounded in the region*

$$\Omega = \left\{ (S(t), S_L(t), I(t), I_L(t)) \in \mathbb{R}^4 : \quad N(t) \leq \frac{\Lambda}{\eta} \right\}. \tag{4.6}$$

Proof. The boundedness of the problem (3.1) can be confirmed by adding all equations of the system (3.1). Thus, the result is obtained as follows

$$D^{\alpha_i}_{0+} N(t) = \Lambda - \eta N(t), \quad \text{with} \quad N(0) = N_0 \geq 0. \tag{4.7}$$

The solution of Equation (4.7) can be expressed in the form

$$N(t) \leq N_0 \exp(-nt) + \frac{\Lambda}{\eta}(1 - \exp(-nt)). \tag{4.8}$$

It is evident from Equation (4.8) that as $t \longrightarrow \infty$, $N(t) \leq \dfrac{\Lambda}{\eta}$. This implies that the feasible region for the given model can be expressed as follows

$$\Omega = \left\{ (S(t), S_L(t), I(t), I_L(t)) \in \mathbb{R}^4 : \quad N(t) \leq \frac{\Lambda}{\eta} \right\}. \tag{4.9}$$

Hence, the solution of the system (3.1) is bounded. □

4.2. **Existence and uniqueness results for the second proposed model.** In this section, the uniqueness and existence of solutions for the proposed model will be discussed using fixed-point theorems.
The proposed model in Equation (3.3) can be simplified using the following formulation.
Let $\boldsymbol{\alpha} = (\alpha_1, \cdots, \alpha_n)$ and $\alpha_i \in \mathbb{T}$, where $\mathbb{T} = (0, 1]$. We have

$$\begin{cases} D^{\alpha_i}_{0+} S(t) = G_1(t, S(t), S_L(t), I(t), I_L(t), L(t)), \\ D^{\alpha_i}_{0+} S_L(t) = G_2(t, S(t), S_L(t), I(t), I_L(t), L(t)), \\ D^{\alpha_i}_{0+} I(t) = G_3(t, S(t), S_L(t), I(t), I_L(t), L(t)), \\ D^{\alpha_i}_{0+} I_L(t) = G_4(t, S(t), S_L(t), I(t), I_L(t), L(t)), \\ D^{\alpha_i}_{0+} L(t) = G_5(t, S(t), S_L(t), I(t), I_L(t), L(t)), \end{cases} \tag{4.10}$$

where

$$\begin{cases} G_1(t,S(t),S_L(t),I(t),I_L(t),L(t)) = \Lambda^{\alpha_i} - \beta^{\alpha_i} S(t)I(t) - \lambda_1^{\alpha_i} S(t)L(t) - d^{\alpha_i} S(t) + \gamma_1^{\alpha_i} I(t) \\ +\gamma_2^{\alpha_i} I_L(t) + \theta_1^{\alpha_i} S_L(t), \\ G_2(t,S(t),S_L(t),I(t),I_L(t),L(t)) = \lambda_1^{\alpha_i} S(t)L(t) - d^{\alpha_i} S_L(t) - \theta_1^{\alpha_i} S_L(t), \\ G_3(t,S(t),S_L(t),I(t),I_L(t),L(t)) = \beta^{\alpha_i} S(t)I(t) - \gamma_1^{\alpha_i} I(t) - \nu_1^{\alpha_i} I(t) - d^{\alpha_i} I(t) + \lambda_2^{\alpha_i} I(t)L(t) \\ +\theta_2^{\alpha_i} L(t), \\ G_4(t,S(t),S_L(t),I(t),I_L(t),L(t)) = \lambda_2^{\alpha_i} I(t)L(t) - d^{\alpha_i} I_L(t) - \theta_2^{\alpha_i} I_L(t) - \gamma_2^{\alpha_i} I_L(t) - \nu_2^{\alpha_i} I_L(t), \\ G_5(t,S(t),S_L(t),I(t),I_L(t),L(t)) = \mu^{\alpha_i} I(t) - \phi^{\alpha_i}. \end{cases} \tag{4.11}$$

Therefore, the proposed model in Equation (3.3) can be formulated as follows

$$\begin{cases} D_0^{\alpha_i}\phi(t) = \mathcal{K}(t,\phi(t)), \quad t \in J = [0,b], \quad \alpha = (\alpha_1,\cdots,\alpha_n), \quad 0 < \alpha_i \leq 1, \\ \phi(0) = \phi_0 \geq 0. \end{cases} \tag{4.12}$$

On the condition that

$$\begin{cases} \phi(t) = (S(t),S_L(t),I(t),I_L(t),L(t))^T, \\ \phi(0) = (S_0,S_{L_0},I_0,I_{L_0},L_0)^T \\ \mathcal{K}(t,\phi(t)) = (G_j(S(t),S_L(t),I(t),I_L(t),L(t)))^T, \quad j = 1,\cdots,5, \end{cases} \tag{4.13}$$

where $(.)^T$ denotes the transpose operation. Referring to Lemma 4.1, the integral corresponding to the stated issue in (4.12), which is equal to model (4.12), is shown as follows

$$\begin{aligned} \phi(t) &= \phi_0 + I_{0^+}^{\alpha_i}\mathcal{K}(t,\phi(t)) \\ &= \phi_0 + \frac{1}{\Gamma(\alpha_i)}\int_0^t (t-x)^{\alpha_i - 1}\mathcal{K}(x,\phi(x))dx, \quad \boldsymbol{\alpha} = (\alpha_1,\cdots,\alpha_n), \quad \alpha_i \in \mathbb{T}, \quad \mathbb{T} = (0,1], \\ \phi(t) &= \phi_0 + \lim_{h\longrightarrow 0} \frac{\mathcal{K}\Big((x,\phi(x)) + h(x,\phi(x))^{1-\alpha_i}\Big) - \mathcal{K}(x,\phi(x))}{h}. \end{aligned} \tag{4.14}$$

The Banach space E is defined as $C([0,b],\mathbb{R})$, which consists of all continuous functions mapping from $[0,b]$ to $\mathbb{R}$. The norm on $\mathbb{E} = C([0,b],\mathbb{R})$ is defined as follows

$$\|\phi\|_{\mathbb{E}} = \sup_{t\in J} |\phi(t)|, \tag{4.15}$$

where

$$|\phi(t)| = |S(t)| + |S_L(t)| + |I(t)| + |I_L| + |L(t)|, \tag{4.16}$$

and $S, S_L, I, I_L, L \in C([0,b],\mathbb{R})$.

Proposition 4.4. *Assume that the function $\mathcal{K} \in C([J,\mathbb{R}])$ is required to map a bounded subset of $J \times \mathbb{R}^5$ to subsets that are relative to $\mathbb{R}$. Also, there exists a constant $\mathcal{L}_{\mathcal{K}} > 0$ such that*

$$|\mathcal{K}(t,\phi_1(t)) - \mathcal{K}(t,\phi_2(t))| \leq \mathcal{L}_{\mathcal{K}}|\phi_1(t) - \phi_2(t)|, \tag{4.17}$$

for all $t \in J$ and every $\phi_1, \phi_2 \in C([J,\mathbb{R}])$.
Then, the problem (4.12), which is equivalent to the proposed model (3.3), has a unique solution provided that $\Sigma\mathcal{L}_{\mathcal{K}} < 1$, where

$$\Sigma = \frac{b^{\alpha_i}}{\Gamma(\alpha_i + 1)}. \tag{4.18}$$

Proof. Assume that the operator $P : \mathbb{E} \longrightarrow \mathbb{E}$ is defined as follows

$$(P\phi)(t) = \phi_0 + \frac{1}{\Gamma(\alpha_i)} \int_0^t (t-x)^{\alpha_i - 1} \mathcal{K}\left(x, \phi(x)\right) dx\cdot$$

Therefore

$$(P\phi)(t) = \phi_0 + \lim_{h \longrightarrow 0} \frac{\mathcal{K}\left((x,\phi(x)) + h\left(x,\phi(x)\right)^{1-\alpha_i}\right) - \mathcal{K}\left((x,\phi(x))\right)}{h}$$

Clearly, the operator P is well-defined and represents a unique solution of model (3.3), which is commonly referred to as a fixed point of P.
In fact, it is assumed that $\sup_{t\in J} \|\mathcal{K}(t,0)\| = M_1$ and $K \geq \|\phi_0\| + \Sigma M_1$.
So, it is sufficient to indicate that $P\mathbb{B}_K \subset \mathbb{B}_K$, where the set $\mathbb{B}_K = \{\phi \in \mathbb{E} : \ \|\phi\| \leq K\}$ is both closed and convex. Now, for any $\phi \in \mathbb{B}_{\mathcal{K}}$, we have

$$\begin{aligned}
|(P\phi)(t)| &\leq |\phi_0| + \lim_{h\longrightarrow 0}\left(\frac{\mathcal{K}\left((x,\phi(x)) + h\left(x,\phi(x)\right)^{1-\alpha_i}\right) - \mathcal{K}\left((x,\phi(x))\right)}{h}\right) \\
&\leq \phi_0 + \lim_{h\longrightarrow 0}\Bigg|\frac{\left[\mathcal{K}\left((x,\phi(x)) + h\left(x,\phi(x)\right)^{1-\alpha_i}\right) - \mathcal{K}\left((x,\phi(x))\right)\right]}{h} \\
&- \frac{\left[\mathcal{K}\left((x,0) + h(x,0)^{1-\alpha_i}\right) - \mathcal{K}\left((x,0)\right)\right]}{h}\Bigg| + \left|\frac{\mathcal{K}\left((x,0) + h(x,0)^{1-\alpha_i}\right)}{h}\right| \\
&\leq \phi_0 + \Sigma(\mathcal{L}_{\mathcal{K}} K + M_1) \leq K\cdot
\end{aligned} \tag{4.19}$$

Hence, the outcomes follow. Additionally, for any given $\phi_1, \phi_2 \in \mathbb{E}$, we obtain

$$\begin{aligned}
|(P\phi_1)(t) - (P\phi_2)(t)| &\leq \lim_{h\longrightarrow 0}\Bigg|\frac{\left[\mathcal{K}\left((x,\phi_1(x)) + h\left(x,\phi_1(x)\right)^{1-\alpha_i}\right)\right.}{h} - \frac{\left.\mathcal{K}\left((x,\phi_1(x))\right)\right]}{h} \\
&- \left(\lim_{h\longrightarrow 0}\Bigg|\frac{\left[\mathcal{K}\left((x,\phi_2(x)) + h\left(x,\phi_2(x)\right)^{1-\alpha_i}\right)\right.}{h} - \frac{\left.\mathcal{K}\left((x,\phi_2(x))\right)\right]}{h}\right)\Bigg| \\
&\leq \mathcal{L}_{\mathcal{K}} \lim_{h\longrightarrow 0}\Bigg|\frac{\left[\phi_2(x + hx^{1-\alpha_i}) - \phi_2(x)\right]}{h} \\
&- \frac{\left[\phi_2(x + hx^{1-\alpha_i}) - \phi_2(x)\right]}{h}\Bigg| \leq \Sigma\mathcal{L}_{\mathcal{K}}|\phi_1(t) - \phi_2(t)|,
\end{aligned} \tag{4.20}$$

which implies that

$$\|(P\phi_1) - (P\phi_2)\| \leq \Sigma\mathcal{L}_{\mathcal{K}}\|\phi_1 - \phi_2\|\cdot \tag{4.21}$$

Therefore, as a consequence of the Banach contraction, the proposed model (3.3) has a unique solution. □

Remark 4.5. To express the next lemma and theorem, the following assumption is required.
Assume that there exist $\delta_1, \delta_2 \in \mathbb{E}$ such that $|\mathcal{K}(t,\phi(t))| \leq \delta_1(t) + \delta_2|\phi(t)|$ for any $\phi \in \mathbb{E}$ and $t \in J$.
In which,

$$\delta_1^* = \sup_{t\in J}|\delta_1(t)|, \quad \delta_2^* = \sup_{t\in J}|\delta_2(t)| < 1\cdot \tag{4.22}$$

Lemma 4.6. *The operator P defined in (4.19) is completely continuous.*

Proof. Evidently, the continuity of the operator P is obtained from the continuity of the function $\mathcal{K}$. Thus, for any $\phi \in \mathbb{B}_{\mathcal{K}}$, as defined above, we have

$$\begin{aligned}
|(P\phi)(t)| &= \left|\phi_0 + \lim_{h\longrightarrow 0} \frac{\mathcal{K}\left((x,\phi(x)) + h(x,\phi(x))^{1-\alpha_i}\right) - \mathcal{K}\left(x,\phi(x)\right)}{h}\right| \\
&\leq \|\phi_0\| + \lim_{h\longrightarrow 0} \frac{\mathcal{K}\left((x,\phi(x)) + h(x,\phi(x))^{1-\alpha_i}\right) - \mathcal{K}\left(x,\phi(x)\right)}{h} \\
&= \|\phi_0\| + \frac{1}{\Gamma(\alpha_i)}\int_0^t (t-x)^{(\alpha_i)-1}|\mathcal{K}(x,\phi(x))|dx \\
&\leq \|\phi_0\| + \frac{(\delta_1^* + \delta_2^*\|\phi\|)}{\Gamma(\alpha_i)}\int_0^t (t-x)^{(\alpha_i)-1}dx \\
&\leq \|\phi_0\| + \frac{(\delta_1^* + \delta_2^*\|\phi\|)}{\Gamma(\alpha_i)} b^{(\alpha_i)} = \|\phi_0\|\Sigma(\delta_1^* + \delta_2^*\|\phi\|) < +\infty\cdot
\end{aligned} \tag{4.23}$$

As a result, it can be said that the operator P is uniformly bounded. Then, the equicontinuity of P will be proved. To achieve this goal, we proceed as follows

$$\sup_{(t,\phi)\in J\times\mathbb{B}_{\mathcal{K}}} |\mathcal{K}(t,\phi(t))| = \mathcal{K}^*\cdot \tag{4.24}$$

Next, for every $t_1, t_2 \in J$ where $t_2 \geq t_1$, it follows that

$$\begin{aligned}
|(P\phi)(t_2) - (P\phi)(t_1)| &= \frac{1}{\Gamma(\alpha_i)}\left|\int_0^{t_1}\left[(t_2-x)^{(\alpha_i)-1} - (t_1-x)^{(\alpha_i)-1}\right]\mathcal{K}(x,\phi(x))dx\right. \\
&+ \left.\int_{t_1}^{t_2}(t_2-x)^{(\alpha_i)-1}\mathcal{K}(x,\phi(x))dx\right| \\
&\leq \frac{\mathcal{K}^*}{\Gamma(\alpha_i)}[2(t_2-t_1)^{(\alpha_i)} + (t_2^{(\alpha_i)} - t_1^{(\alpha_i)})] \longrightarrow 0,
\end{aligned} \tag{4.25}$$

as $t_2 \longrightarrow t_1$. □

We can conclude that the operator P is equicontinuous and, consequently, relatively compact on $\mathbb{B}_{\mathcal{K}}$. Therefore, we can conclude that P is completely continuous as a result of the Arzela-Ascoli theorem.

Proposition 4.7. *Let's assume that the function $\mathcal{K} : J \times \mathbb{R}^5 \longrightarrow \mathbb{R}$ is a continuous function that satisfies the assumption stated in (4.22). Therefore, the problem stated in (4.12), which is equivalent to the proposed model (3.3), will have at least one solution.*

Proof. A set has been defined as follows

$$\mathcal{U} = \{\phi \in \mathbb{E} : \ \phi = \epsilon(P\phi)(x), \ 0 < \epsilon < 1\}\cdot \tag{4.26}$$

Clearly, by considering Lemma 4.6, the operator $P : \mathcal{U} \longrightarrow \mathbb{E}$ is completely continuous as defined in (4.19). Now, for any $\phi \in \mathcal{U}$ and leveraging the advantage of assumption (4.22), it is obtained that

$$\begin{aligned}
|\phi(t)| &= |\epsilon(P\phi)(t)| \\
&\leq |\phi_0| + \lim_{h\longrightarrow 0}\left|\frac{\left[\mathcal{K}\left((x,\phi(x)) + h(x,\phi(x))^{1-\alpha_i}\right)\right]}{h} - \frac{\mathcal{K}((x,\phi(x)))}{h}\right| \\
&= |\phi_0| + \frac{1}{\Gamma(\alpha_i)}\int_0^t (t-x)^{\alpha_i-1}|\mathcal{K}(x,\phi(x))|dx \leq \|\phi_0\| + \frac{(\delta_1^* + \delta_2^*\|\phi\|)}{\Gamma(\alpha_i+1)} b^{\alpha_i} \\
&= \|\phi_0\| + \Sigma(\delta_1^* + \delta_2^*\|\phi\|) < +\infty\cdot
\end{aligned} \tag{4.27}$$

□

Therefore, the related set $\mathcal{U}$ is bounded. Thus, the operator P possesses at least one fixed point, which can be considered as the solution of the proposed model (3.3). As a result, this is the desired outcome.

5. Analysis and stability result

This section comprises two parts. The first part includes the possible fixed point and an analysis of the local stability concerning the suggested model (3.1) Figure 1.
The second part involves the derivation of the stability of the proposed model (3.3).

5.1. **Equilibrium points, basic reproduction number and local stability analysis.** In this section, a possible fixed point of the model (3.1) will be derived. Two feasible equilibrium points have been calculated. The first equilibrium point is associated with the disease-free equilibrium (DFE), and the second equilibrium point is the endemic equilibrium (EE).

$$\begin{aligned} &\lim_{h\longrightarrow 0}\frac{\|S(t+ha^{1-\alpha_i}-S(a))\|}{\|h\|}=\lim_{h\longrightarrow 0}\frac{\|S_l(t+ha^{1-\alpha_i}-S_L(a))\|}{\|h\|}=\\ &\lim_{h\longrightarrow 0}\frac{\|I(t+ha^{1-\alpha_i}-I(a))\|}{\|h\|}=\lim_{h\longrightarrow 0}\frac{\|I_L(t+ha^{1-\alpha_i}-I_L(a))\|}{\|h\|}=0,\\ \Rightarrow\quad &D_{0^+}^{\alpha_i}S(t)=D_{0^+}^{\alpha_i}S_L(t)=D_{0^+}^{\alpha_i}I(t)=D_{0^+}^{\alpha_i}I_L(t)\cdot \end{aligned} \tag{5.1}$$

By using Equation (5.1), the model (3.1) takes the following form

$$\begin{cases} \dfrac{jS_L(t)I(t)}{N}-\eta S(t)-\psi S(t)=0,\\ \Lambda-\eta S_L(t)-\dfrac{jS_L(t)I(t)}{N}=0,\\ \psi S(t)-\eta I(t)-\omega I(t)=0,\\ \omega I(t)-\eta I_L(t)=0\cdot \end{cases} \tag{5.2}$$

From the state system (5.2), we can deduce the following:
By assuming $S(t)=I(t)=I_l(t)=0$, it can be stated that:

$$\psi_{DFE}=(S_L^0,S^0,I^0,I_L^0)=(\frac{\Lambda_L}{\eta_L},0,0,0), \tag{5.3}$$

$$\psi_{EE}=(S_L^*,S^*,I^*,I_L^*)\cdot \tag{5.4}$$

The basic reproduction number $\mathcal{R}_0$ is evaluated as

$$\mathcal{R}_0=\frac{j\psi}{(\eta+\psi)(\eta+\omega)}\cdot \tag{5.5}$$

Result 5.1. The $DFE\psi^0$ of the system (3.1) is locally asymptotically stable if $\mathcal{R}_0<1$.

5.2. **Stability results.** Here, the stability properties of the proposed model (3.3) will be derived in two well-known frameworks, namely the Ulam-Hyers stability and the stability of the extended Ulam-Hyers. The concept of Ulam stability was defined and considered by Ulam [8].
As stability is crucial for approximate solutions, nonlinear functional analysis has been employed to analyze both the Ulam-Hyers stability and the extended stability of the proposed model (3.3). Therefore, the explanations presented in the following part are necessary.

Definition 5.2. Let $\epsilon>0$, and consider the inequality

$$|D_{0^+}^{\alpha_i}\bar{\phi}(t)-\mathcal{K}(t,\bar{\phi}(t))|\leq\epsilon,\quad t\in J, \tag{5.6}$$

where $\epsilon=\max(\epsilon_j)^T$, $j=1,\cdots,5$.

Definition 5.3. The proposed problem (4.12), which is equivalent to the model (3.3), is Ulam-Hyers stable if $\mathcal{C}_{\mathcal{K}} > 0$ and the function $\varphi_{\mathcal{K}} : \mathbb{R}_+ \to \mathbb{R}_+$ is such that $\varphi_{\mathcal{K}}(0) = 0$. For any $\epsilon > 0$ and for each solution $\bar{\phi} \in \mathbb{E}$ satisfying the inequality (5.6), there exists a solution $\phi \in \mathbb{E}$ of the problem (4.12) such that

$$|\bar{\phi}(t) - \phi(t)| \leq \mathcal{C}_{\mathcal{K}}\epsilon, \quad t \in J, \tag{5.7}$$

where $\mathcal{C}_{\mathcal{K}} = \max(\mathcal{C}_{\mathcal{K}_i})^T$, and

$$|\bar{\phi}(t) - \phi(t)| \leq \varphi_{\mathcal{K}}\epsilon, \quad t \in J, \tag{5.8}$$

where $\varphi_{\mathcal{K}} = \max(\varphi_{\mathcal{K}_i})^T$.

Remark 5.4. A function $\bar{\phi} \in \mathbb{E}$ is a solution of the given inequality (5.6) if and only if there exists a function that satisfies the following conditions

(1) $|h(t)| \leq \epsilon, \qquad h = \max(h_j)^T, \qquad t \in J,$
(2) $D^{\alpha_i}_{0^+}\bar{\phi}(t) = \mathcal{K}(t, \bar{\phi}(t)) + h(t), \qquad t \in J.$

Lemma 5.5. *Assuming that $\bar{\phi} \in \mathbb{E}$ satisfies the inequality (5.6), then $\bar{\phi}$ satisfies the integral inequality described by*

$$\left|\bar{\phi}(t) - \bar{\phi}_0 - \lim_{h\longrightarrow 0}\left[\frac{\left[\mathcal{K}\left((x, \bar{\phi}(x)) + h(x, \bar{\phi}(x))^{1-\alpha_i}\right)\right]}{h} - \frac{\mathcal{K}((x, \bar{\phi}(x)))}{h}\right]\right| \leq \Sigma\epsilon\cdot \tag{5.9}$$

Proof. With reference to item (2) of Remark 5.4, we have

$$D^{\alpha}_{0^+}\bar{\phi}(t) = \mathcal{K}(t, \bar{\phi}(t)) + h(t), \qquad t \in J\cdot, \tag{5.10}$$

and according to Lemma 2.5, it follows that:

$$\bar{\phi}(t) = \bar{\phi}_0 + \lim_{h\longrightarrow 0}\left[\frac{\mathcal{K}((x, \bar{\phi}(x)) + h(x, \bar{\phi}(x))^{1-\alpha_i})}{h} - \frac{\mathcal{K}((x, \bar{\phi}(x)))}{h}\right] + \lim_{k\longrightarrow 0}\frac{h(x + kx^{1-\alpha_i})}{k}\cdot \tag{5.11}$$

The following relation is obtained by using item (1) of Remark 5.4.

$$\left|\bar{\phi}(t) - \bar{\phi}_0 - \lim_{h\longrightarrow 0}\left[\frac{\mathcal{K}\left((x, \bar{\phi}(x)) + h(x, \bar{\phi}(x))^{1-\alpha_i}\right)}{h} - \frac{\mathcal{K}((x, \bar{\phi}(x)))}{h}\right]\right| \leq \lim_{k\longrightarrow 0}\frac{|h(x + kx^{1-\alpha_i}) - h(x)|}{k} \leq \Sigma\epsilon\cdot \tag{5.12}$$

Hence, the expected results are obtained. □

Theorem 5.6. *Suppose that $\mathcal{K} : J \times \mathbb{R}^5 \longrightarrow \mathbb{R}$ is continuous for every $\phi \in \mathbb{E}$, and assumption (4.17) holds with $1 - \Sigma\mathcal{L}_{\mathcal{K}} > 0$.*

$$\begin{aligned}
|\bar{\phi}(t) - \phi(t)| &= \max_{t\in j}\left|\bar{\phi}(t) - \bar{\phi}_0 - \lim_{h\longrightarrow 0}\left[\frac{\mathcal{K}\left((x, \phi(x)) + h(x, \phi(x))^{1-\alpha_i}\right)}{h} - \frac{\mathcal{K}((x, \phi(x)))}{h}\right]\right| \\
&\leq \max_{t\in j}\left|\bar{\phi}(t) - \bar{\phi}_0 - \lim_{h\longrightarrow 0}\left[\frac{\mathcal{K}\left((x, \bar{\phi}(x)) + h(x, \bar{\phi}(x))^{1-\alpha_i}\right)}{h} - \frac{\mathcal{K}((x, \bar{\phi}(x)))}{h}\right]\right| \\
&+ \max_{t\in j}\lim_{h\longrightarrow 0}\left[\frac{\left|\left[\mathcal{K}\left((x, \bar{\phi}(x)) + h(x, \bar{\phi}(x))^{1-\alpha_i}\right)\right]\right|}{h} - \frac{\mathcal{K}[(x, \bar{\phi}(x))]}{h}\right] \\
&- \left[\frac{\mathcal{K}\left((x, \phi(x)) + h(x, \phi(x))^{1-\alpha_i}\right)}{h} - \frac{\mathcal{K}((x, \phi(x)))}{h}\right] \\
&\leq \left|\phi(t) - \bar{\phi}_0 - \lim_{h\longrightarrow 0}\left[\frac{\mathcal{K}\left((x, \bar{\phi}(x)) + h(x, \bar{\phi}(x))^{1-\alpha_i}\right)}{h} - \frac{\mathcal{K}((x, \bar{\phi}(x)))}{h}\right]\right| \\
&+ \mathcal{L}_{\mathcal{K}}\lim_{h\longrightarrow 0}\left|\frac{[\bar{\phi}(x + hx^{1-\alpha_i})]}{h}\right. \\
&- \left.\frac{[\phi(x + hx^{1-\alpha_i},) - \phi(x)]}{h}\right| \leq \Sigma\epsilon + \Sigma\mathcal{L}_{\mathcal{K}}|\bar{\phi}(t) - \phi(t)|\cdot
\end{aligned} \tag{5.13}$$

Therefore, $\left||\bar{\phi}-\phi|\right| \leq \mathcal{C}_{\mathcal{K}}\epsilon$, *where* $\mathcal{C}_{\mathcal{K}} = \dfrac{\Sigma}{1-\Sigma\mathcal{L}_{\mathcal{K}}}$.

By setting $\varphi_{\mathcal{K}}(\epsilon) = \mathcal{C}_{\mathcal{K}}\epsilon$, such that $\varphi_{\mathcal{K}}(0) = 0$, it can be concluded that the proposed problem (3.3) is stable in both the Ulam-Hyers framework and the generalized Ulam-Hyers framework.

6. Numerical scheme and simulations

In this section, the numerical simulation of the fractional variant for the current model, investigated utilizing the $\boldsymbol{\alpha}$-fractional operator, has been conducted using first-order convergent numerical techniques.

We consider the following fractional variant of the model.

$$ {}^{*}D^{\alpha_i}_{0,x}(y(t)) = g(y(t)), \quad \alpha_i \in (0,1), \quad \boldsymbol{\alpha} = (\alpha_1, \cdots, \alpha_n), \quad x \in [0,T], \quad y(0) = y_0, \tag{6.1}$$

where $y = (a, b, c, w) \in \mathbb{R}^4_+$ is a real-valued continuous vector function that satisfies the Lipschitz criterion as follows:

$$\|g(y_1(t)) - g(y_2(t))\| \leq M\|(y_1(t)) - (y_2(t))\|, \tag{6.2}$$

where M is a positive real Lipschitz constant.

By utilizing the $\boldsymbol{\alpha}$-fractional-order integral operators, we obtain

$$y(t) = y_0 + I^{\alpha_i}_{0,x}(y(t)), \quad \alpha_i \in (0,1), \quad \boldsymbol{\alpha} = (\alpha_1, \cdots, \alpha_n), \quad x \in [0,T]\cdot \tag{6.3}$$

Here, $I^{\alpha_i}0, x$ represents the α-fractional-order integral operator. Equi-spaced integration intervals over $[0,T]$ with a fixed step size $h = \dfrac{T}{n}$, where $n \in \mathbb{N}$, will be considered. For the simulation, a step size of $h = 10^{-2}$ is utilized.

It is assumed that y_q represents the approximated form of $y(t)$ at $x = x_q$ for $q = 0, 1, \cdots, n$.

In the following equation, a numerical approach has been evaluated to govern the model for the $\boldsymbol{\alpha}$-fractional derivative operator.

$$\begin{aligned}
{}^{c}S_{p+1} &= a_0 + \frac{h^{\alpha_i}}{\Gamma(\alpha_i+1)} \times \sum_{k=0}^{p}((p-k+1)^{\alpha_i} - (p-k)^{\alpha_i})(\Lambda - \beta S(t)I(t) - \lambda_1 S(t)L(t) - dS(t) \\
&+ \gamma_1 I(t) + \gamma_2 I_L(t) + \theta_1 S_L(t)), \\
{}^{c}SL_{p+1} &= b_0 + \frac{h^{\alpha_i}}{\Gamma(\alpha_i+1)} \times \sum_{k=0}^{p}((p-k+1)^{\alpha_i} - (p-k)^{\alpha_i})(\lambda_1 S(t)L(t) - dS_L(t) - \theta_1 S_L(t)), \\
{}^{c}I_{p+1} &= d_0 + \frac{h^{\alpha_i}}{\Gamma(\alpha_i+1)} \times \sum_{k=0}^{p}((p-k+1)^{\alpha_i} - (p-k)^{\alpha_i})(\beta S(t)I - \gamma_1 I(t) - \nu_1 I(t) - dI(t) \\
&+ \lambda_2 I(t)L(t) + \theta_2 I_L(t)), \\
{}^{c}IL_{p+1} &= e_0 + \frac{h^{\alpha_i}}{\Gamma(\alpha_i+1)} \times \sum_{k=0}^{p}((p-k+1)^{\alpha_i} - (p-k)^{\alpha_i})(\lambda_2 I(t)L(t) - dI_L(t) - \theta_2 I_L(t) \\
&- \gamma_2 I_L(t) - \nu_2 I_L(t)), \\
{}^{c}L_{p+1} &= d_0 + \frac{h^{\alpha_i}}{\Gamma(\alpha_i+1)} \times \sum_{k=0}^{p}((p-k+1)^{\alpha_i} - (p-k)^{\alpha_i})(\mu I(t) - \phi L(t))\cdot
\end{aligned} \tag{6.4}$$

Now, the numerical results obtained from the governing model will be discussed in relation to the approximate solutions. The α-fractional operator has been utilized to achieve this objective. The following are the initial conditions for the problem.

$$S(0) = 900, \quad S_L(0) = 300, \quad I(0) = 300, \quad I_L(0) = 497, \quad L(0) = 200, \tag{6.5}$$

and

$$\alpha_1 = 0.16, \quad \alpha_2 = 0.22, \quad \alpha_3 = 0.33, \quad \alpha_4 = 0.76, \quad \alpha_5 = 0.89\cdot \tag{6.6}$$

In Table 1, the parameter values are displayed. Figure 2 shows the dynamical and representative view of each variable

TABLE 1. Details of parameter values.

parameters	$\alpha_1 = 0.16$/values	$\alpha_2 = 0.22$/values	$\alpha_3 = 0.33$/values	$\alpha_4 = 0.76$/values	$\alpha_5 = 0.89$/values
Λ	1600	1200	800	400	276
β	0.000068	0.000051	0.000034	0.000017	0.0000114
λ_1	0.0008	0.0006	0.0004	0.0002	0.00013
λ_2	0.0008	0.0006	0.0004	0.0002	0.00013
ν_1	0.131	0.09825	0.0655	0.03275	0.02183
ν_2	0.131	0.09825	0.0655	0.03275	0.02183
d	0.0384	0.0288	0.0192	0.0096	0.0064
θ_1	0.8	0.6	0.4	0.2	0.13
θ_2	0.8	0.6	0.4	0.2	0.13
μ	0.002	0.0015	0.001	0.0005	0.00033
ϕ	0.24	0.18	0.12	0.06	0.04
γ_1	0.67916	0.50937	0.33958	0.16979	0.11319
γ_2	0.67916	0.50937	0.33958	0.16979	0.11319

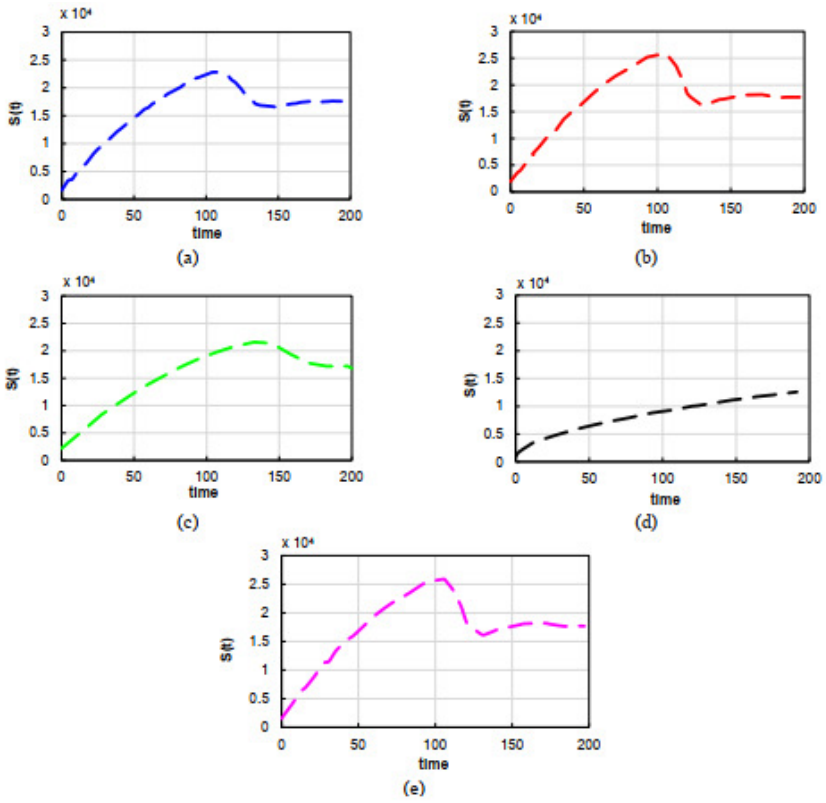

FIGURE 2. Dynamical outlook of the susceptible class that is n't under lockdown and susceptible class that is under lockdown with different $\boldsymbol{\alpha}$-fractional-order values.

for various α-fractional order values. In the plots depicted below, the susceptible class, $S(t)$, indicates the behavior of increment and decrement. It is also noteworthy that lower values of $\boldsymbol{\alpha}$ lead to a diminishing decreasing rate and an increasing rate that becomes higher. With the same values as those seen in the following Figure 3, the susceptible class under lockdown, $S_L(t)$, also exhibits increasing-decreasing behavior with lower values of $\boldsymbol{\alpha}$. Furthermore, the decreasing rate also begins to disappear. In Figure 4 below, the infected class, denoted as $I(t)$, exhibits a noticeable

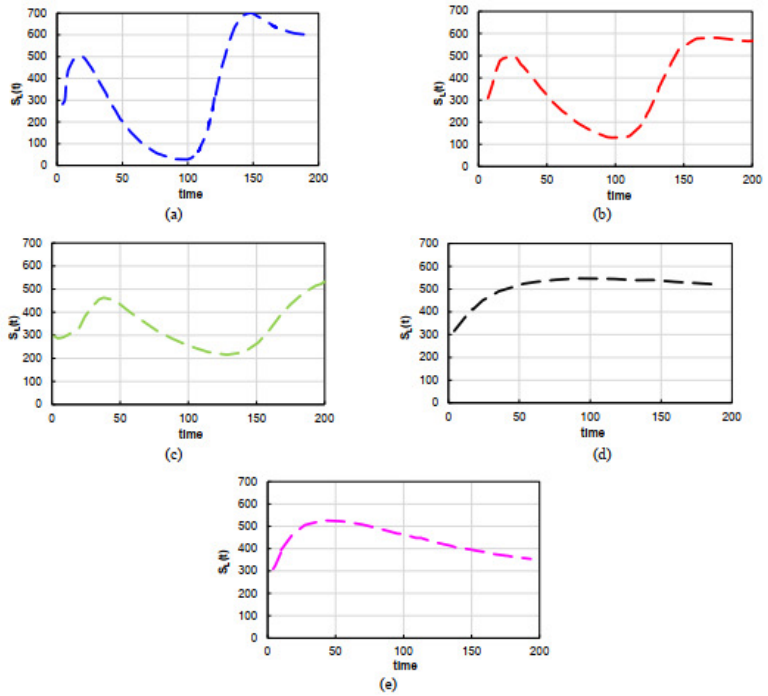

FIGURE 3. Dynamical outlook of the infective class that isn't under lockdown and infective class those are under lockdown with different $\boldsymbol{\alpha}$-fractional-order values.

increasing-decreasing pattern. As lower fractional-order values are employed, the class achieves complete stability.

In the figure depicted below, the infected class under lockdown, $I_L(t)$, maintains a distinct increasing-decreasing pattern. However, it is noteworthy that the class is likely at risk.

In the plots below, the dynamic outlook of the population under lockdown, $L(t)$, is illustrated. An increasing behavior is observed. There seems to be a strong trend in this case, which may be associated with the risks concerning the class. With many individuals infected under lockdown, including both asymptomatic and symptomatic cases, there could be an increase in the death rate, resulting in a significant decrease in the number of people under lockdown.

7. Conclusions

In conclusion, we have investigated a system of nonlinear fractional-order equations within the framework of $\boldsymbol{\alpha}$-fractional calculus to evaluate the effectiveness of lockdown measures in mitigating the spread of Coronavirus. The uniqueness and existence of solutions for the proposed Coronavirus model under lockdown were established using fixed-point theorems such as Schauder and Banach. Stability analysis was conducted using the Ulam-Hyers and extended Ulam-Hyers frameworks. Additionally, numerical simulations of the fractional variant of the model were performed utilizing fractional operators. The simulations employed the method of fractional Euler, a first-order convergent numerical technique. The behavior and dynamics of each variable were explored across different fractional-order values.

Our study reveals that the depiction and dynamic behavior of each variable vary significantly with changes in $\boldsymbol{\alpha}$-fractional order values. Specifically:

(1) The susceptible class, $S(t)$, displays an oscillatory pattern of increase and decrease. Notably, at lower values of $\boldsymbol{\alpha}$, the rate of decrease diminishes, while the rate of increase intensifies.

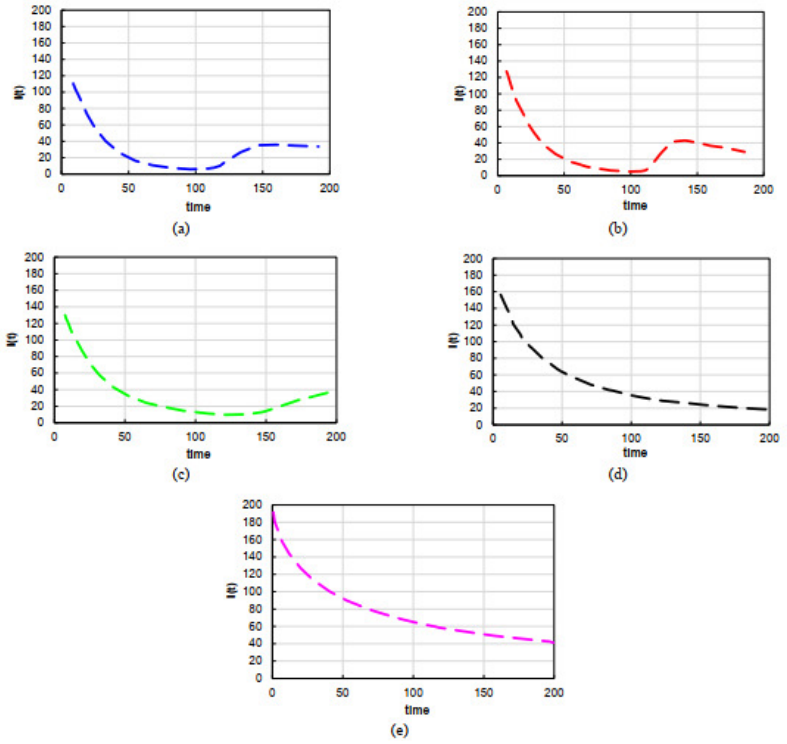

FIGURE 4. Dynamical outlook of the commutative density of the lockdown class with different $\boldsymbol{\alpha}$-fractional-order values.

(2) The susceptible class under lockdown, $S_L(t)$, also exhibits oscillatory behavior, with a diminishing rate of decrease observed at lower fractional-order values.
(3) The infected class, $I(t)$, demonstrates a similar oscillatory pattern, with lower fractional-order values leading to greater stability in the class dynamics.
(4) The infected class under lockdown, $I_L(t)$, maintains an oscillatory pattern similar to $I(t)$, but with an increased risk observed, particularly at lower fractional-order values.

Overall, our findings underscore the nuanced impact of fractional-order values on the dynamics of the Coronavirus model under lockdown, highlighting the importance of considering such factors in assessing disease containment strategies.

REFERENCES

[1] T. Chen, J. Rui, Q. Wang, Z. Zhao, J. Cui, and L. Yin, *A mathematical model for simulating the transmission of Wuhan novel Coronavirus*, bioRxiv, (2020).
[2] D. Fargette et al., *Diversification of rice yellow mottle virus and related viruses spans the history of agriculture from the neolithic to the present*, PLos pathogens, *4* (2008), e1000125.
[3] A. A. Kilbas, H. M. Srivastava, and J. J. Trujillo, *Theory and applications of fractional differential equations*, Elsevier, (2006).
[4] R. Khalil, M. Al Horani, A. Yousef and M. Sababheh, *A new definition of fractional derivative*, Journal of Computational and Applied Mathematics, *264* (2014), 65-70.
[5] H. Khan, J. Gómez-Aguilar, A. Alkhazzan, and A. Khan, *A fractional order HIV-TB coinfection model with nonsingular Mittag-Leffler Law*, Mathematical Methods in the Applied Sciences, *43* (2020), 3786-3806.

[6] M. A. Khan and A. Atangana, *Modeling the dynamics of novel coronavirus (2019-nCov) with fractional derivative*, Alexandria Engineering Journal, *59* (2020), 2379-2389.
[7] A. J. McMichael, *Environmental and social influences on emerging infectious diseases: past, present and future*, Philosophical Transactions of the Royal Society of London, Series B: Biological Sciences, *359* (2004), 1049-1058.
[8] K. Shah, M. A. Alqudah, F. Jarad, and T. Abdeljawad, *Semi-analytical study of Pine Wilt Disease model with convex rate under Caputo–Febrizio fractional order derivative*, Chaos, Solitons, Fractals, *135* (2020), 109754.
[9] K. Shah, F. Jarad, and T. Abdeljawad, *On a nonlinear fractional order model of dengue fever disease under Caputo-Fabrizio derivative*, Alexandria Engineering Journal, *59* (2020), 2305-2313.
[10] A. S. Shaikh, I. N. Shaikh, and K. S. Nisar, *A mathematical model of COVID-19 using fractional derivative: outbreak in India with dynamics of transmission and control*, Advances in Difference Equations, *2020* (2020), 1-19.
[11] E. Tognotti, *Lessons from the history of quarantine, from plague to influenza A*, Emerging infectious diseases, *19*(2) (2013), 254.
[12] R. Ud Din, K. Shah, I. Ahmad, and T. Abdeljawad, *Study of transmission dynamics of novel COVID-19 by using mathematical model*, Advances in Difference Equations, *2020* (2020), 1-13.
[13] C. Xu, Y. Yu, Y. Chen, and Z. Lu. Forecast analysis of the epidemics trend of COVID-19 in the USA by a generalized fractional-order SEIR model. Nonlinear dynamics, *101* (2020), 1621-1634.
[14] M. Yousaf, S. Zahir, M. Riaz, S. M. Hussain, and K. Shah, *Statistical analysis of forecasting COVID-19 for upcoming month in Pakistan*, Chaos, Solitons, Fractals, *138* (2020), 109926.